Digital Twin-Based Heat Stress Monitoring System in Construction

Yoojun Kim[1] and Youngjib Ham, Ph.D., A.M.ASCE[2]

[1]Ph.D. Student, Dept. of Construction Science, Texas A&M Univ., TX.
Email: yoojun@tamu.edu
[2]History Maker Homes Endowed Associate Professor, Dept. of Construction Science, Texas A&M Univ., TX. Email: yham@tamu.edu

ABSTRACT

Construction work exposes workers to high levels of heat, which poses significant risks to their occupational health. In order to mitigate these risks, it is crucial to have a thorough understanding of the heat exposure that workers face. This study proposes a novel framework that leverages the combination of UAV photogrammetry and microclimate simulation to address the previously overlooked risks associated with heat radiation at construction sites. A case study was conducted in College Station, TX, in July 2022, to validate the effectiveness of the proposed framework. The results emphasize the significance of monitoring site-scale radiant heat-induced risks, while conventional indicators like air temperature and heat index do not fully capture the complexities and hazards posed by heat radiation in construction environments.

INTRODUCTION

The construction industry poses a high risk of heat stress to its workers due to the physically demanding nature of the work and frequent exposure to outdoor environments (Acharya et al. 2018). The US Census of Fatal Occupational Injuries reported that the construction industry has accounted for over a third of all heat-related occupational fatalities from 1992 to 2016 (Dong et al. 2019). To mitigate heat stress, it is crucial to assess its extent by considering four meteorological factors, such as air temperature (T_a), relative humidity (RH), air velocity (V_a), and heat radiation, which collectively impact a worker's heat-related load (Huang et al. 2022; Lai et al. 2014). Of these factors, heat radiation is particularly important, as it significantly impacts human energy balance in outdoor environments, especially during hot summers (Chen et al. 2016). Nevertheless, measuring heat radiation levels in outdoor environments is challenging due to the spatial variations caused by shading effects and the varying thermophysical properties of surface materials (Kántor and Unger 2011).

Prior works in construction have primarily focused on assessing the thermal conditions at specific locations through on-site measurements of heat radiation (Chan et al. 2012; Fang et al. 2021; Szer et al. 2022; Wong et al. 2014; Yi et al. 2016). This approach provides valuable information on momentary heat radiation levels at selected locations, but it is limited in scope and susceptible to uncertainties caused by spatial variations of heat radiation (Lau et al. 2016). As a result, the impact of heat radiation on the health and safety of construction workers remains largely unknown. This limited comprehension is attributable to the challenges involved in obtaining comprehensive information about heat radiation at construction sites. These challenges include logistical and cost constraints associated with multiple on-site measurements, as well as the need for frequent modifications to measurements to account for the dynamic nature of construction environments. To address these limitations, this study proposes a framework for

spatial analysis of heat radiation that incorporates unmanned aerial vehicle (UAV) photogrammetry and microclimate simulation. This framework, which supplements the current on-site measurement methods, takes into account both site geometric features and meteorological conditions to provide a more comprehensive understanding of heat radiation in construction sites. The effectiveness of the proposed framework was validated through a case study conducted in College Station, TX in July 2022. The results of the case study are presented and discussed, emphasizing the importance of the proposed framework for heat risk management in construction.

UNCOVERING THE IMPACT OF HEAT RADIATION IN CONSTRUCTION

This paper aims to address the challenge of spatially varying heat radiation risks in construction sites. The proposed framework involves three key stages: data collection, data processing, and data analysis, as depicted in Figure 1. In the first stage, meteorological data and site images are collected. In the second stage, the collected site images are further processed, and microclimate simulation is performed to estimate the spatially varied mean radiant temperature (T_{mrt}), a critical parameter for assessing heat radiation risks. In the final stage, site-scale heat risks are evaluated using thermo-physiological models.

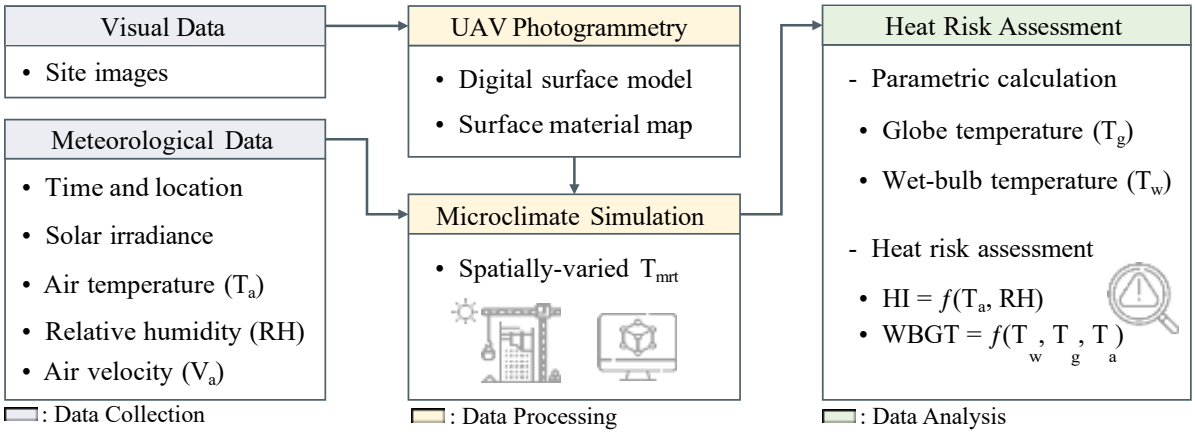

Figure 1. Overview of the proposed framework.

GEOMETRIC DATA CAPTURE USING UAV PHOTOGRAMMETRY

The digital surface model (DSM) is an essential element in capturing site geometry needed for microclimate simulation. However, the constantly evolving site geometry of construction sites presents challenges in obtaining DSM data. To address this challenge, this study leverages UAV photogrammetry, which generates 3D representations of scenes using 2D images taken by a UAV-mounted camera, as shown in Figure 2. Once site images are collected by a UAV, they are utilized to reconstruct a 3D geometric digital twin of the site. Based on this model, the DSM is generated, which is crucial in estimating shade patterns, sky view factors, and ground view factors. To further enhance the accuracy of microclimate simulation, a surface material map is registered based on the DSM. This map is used to estimate longwave radiation fluxes associated with surface materials and vertical walls of built environments in microclimate simulation.

Figure 2. Procedures for site geometry data acquisition.

HEAT RADATION ANALYSIS USING MICROCLIMATE SIMULATION

The microclimate model used in this study, Solar and LongWave Environmental Irradiance Geometry (SOLWEIG), is an established simulation model with validated performance in numerous studies such as (Lindberg et al. 2008). SOLWEIG simulation requires four input data types: (1) time and location data (e.g., geographic coordinate, time of day); (2) meteorological data (T_a, Global Horizontal Irradiance (GHI), and RH); (3) DSM; and (4) surface material map. Using this input data, the model calculates the shortwave-induced radiant flux by considering the solar irradiance and site geometry that generates shading effects, as well as the longwave-induced radiant flux by considering the thermophysical properties of surface materials registered in the surface material map. The six-directional method is utilized to determine the mean radiant flux density, which takes into account both the short and longwave-induced radiant fluxes of the human body. The outcome of the microclimate simulation is the spatially-varying T_{mrt}, calculated using the Stephan-Boltzmann law. The calculation mechanisms are explained in (Lindberg and Grimmond 2011; Lindberg et al. 2016).

HEAT STRESS ASSESSMENT USING HEAT INDEX AND WBGT

The Heat Index (HI) is a widely used thermo-physiological model in the US construction industry because it can be calculated without information on heat radiation. According to the CPL 03-00-024 directive, employers in the US are required to implement managerial measures in response to heat warnings based on the HI by the National Weather Service (NWS). The HI is calculated based on T_a and RH using Equations (1-4) proposed by NWS:

$$\begin{aligned} HI = -42.379 + 2.04901523T_a + 10.14333127RH - 0.22475541T_aRH \\ - 000683783{T_a}^2 - 0.05481717RH^2 + 0.00122874{T_a}^2RH \\ + 0.00085282T_aRH^2 - 0.00000199{T_a}^2RH^2 + Adjustment \end{aligned} \quad (1)$$

If RH is below 13% and T_a falls within the range of 80°F to 112°F,

$$Adjustment = -(13 - RH)/4 \times \sqrt{(17 - |T_a - 95|)/17} \quad (2)$$

If RH exceeds 85% and T_a is within the range of 80°F to 87°F,

$$Adjustment = (\mathrm{RH} - 85)/10 \times (87 - \mathrm{T_a})/5 \quad (3)$$

If HI using Equation (1) is less than 80 °F, then the subsequent formula is utilized:

$$\mathrm{HI} = 0.5 \times (\mathrm{T_a} + 61 + ((\mathrm{T_a} - 68) \times 1.2) + (\mathrm{RH} \times 0.094)) \quad (4)$$

When heat radiation information is available, the most commonly used thermo-physiological model in construction is the Wet Bulb Globe Temperature (WBGT) model (Yi et al. 2016). The calculation of WBGT is performed using Equation (5).

$$\mathrm{WBGT} = 0.7\mathrm{T_w} + 0.2\mathrm{T_g} + 0.1\mathrm{T_a} \quad (5)$$

where T_w is the web-bulb temperature and T_g is globe temperature. T_w is determined empirically using the following Equation (6) suggested by (Stull 2011), which takes into account T_a and RH:

$$\mathrm{T_w} = \mathrm{T_a}\arctan[0.151977(\mathrm{RH} + 8.313659)^{0.5}] + \arctan(\mathrm{T_a} + \mathrm{RH}) - \arctan(\mathrm{RH} - 1.676331) + 0.00391838\mathrm{RH}^{1.5}\arctan(0.023101\mathrm{RH}) - 4.686035 \quad (6)$$

Lastly, an Equation (7) from the ISO 7726 standard is used to calculate T_g using the T_{mrt} estimated through the microclimate simulation.

$$\mathrm{T_g}^4 - \mathrm{T_{mrt}}^4 + \frac{1.1\times 10^8 \times \mathrm{V_a}^{0.6}}{\varepsilon \times \mathrm{D}^{0.4}} \times (\mathrm{T_g} - \mathrm{T_a}) = 0 \quad (7)$$

The globe emissivity (ε) is assumed to be 0.95, and the diameter of the globe thermometer (D) is 0.15m in our case study. The quartic equation is solved to obtain T_g.

CASE STUDY

The case study was to investigate the significance of site-scale heat radiation monitoring and to evaluate the efficacy of the proposed framework in an actual construction project. To this end, meteorological data were gathered from the Solcast at the actual construction jobsite located in College Station, TX (30°37′20.2″N, 96°20′58.6″W) in the United States. The collected meteorological data for the study area is presented in Figure 3. The duration of sunshine was approximately 14 hours, with sunrise occurring at 06:34 and sunset at 20:29. The average T_a was 36.2 °C, with a maximum T_a of 39.4 °C at 15:00, and a minimum T_a of 29.9 °C. The average GHI was 544.9 W/m^2, with a maximum GHI of 921.7 W/m^2 at 13:00. In comparison to T_a, GHI varies drastically between 0 and 921.7 W/ m^2 based on the sun's position relative to local standard time (LST). RH gradually declined from 54.4% to 21.8% at 15:00 and then increased to 38.7% at 20:00. V_a was slightly windier after 14:00, with a maximum of 6 m/s at 18:00.

The results of the microclimate simulation are depicted in Figure 4, showing the spatially-varying T_{mrt} in two-hour intervals. The spatial variations in T_{mrt} can be attributed to shading effects from nearby construction objects that obstruct solar irradiance and differences in surface materials. For example, concrete, which is commonly used in construction, is more susceptible to higher longwave radiation fluxes, while vegetation is less prone to such fluxes among the surface materials in SOLWEIG. At 14:00 and 16:00, the T_{mrt} can vary by as much as 46°C between the

minimum and maximum values, which could imply the possible errors in on-site measurements depending on the observation locations. The T_{mrt} intensity is strongly correlated with the GHI trend, which decreases significantly as the sun approaches the horizon. It is important to note that the distribution of T_{mrt} varies with the sun's position, resulting in different shade patterns at different times. In highly-dense areas, surrounding built environments exert a greater influence on shade patterns, making this variability even more pronounced.

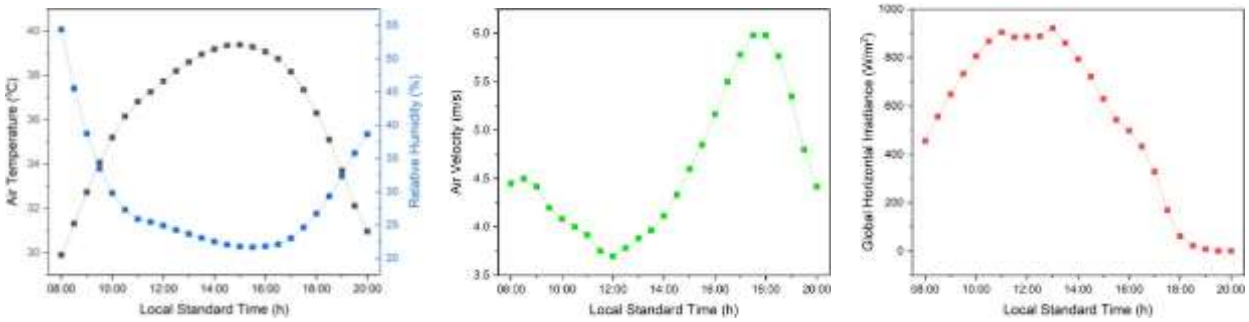

Figure 3. Meteorological conditions on 7/17/2022 (8:00~20:00).

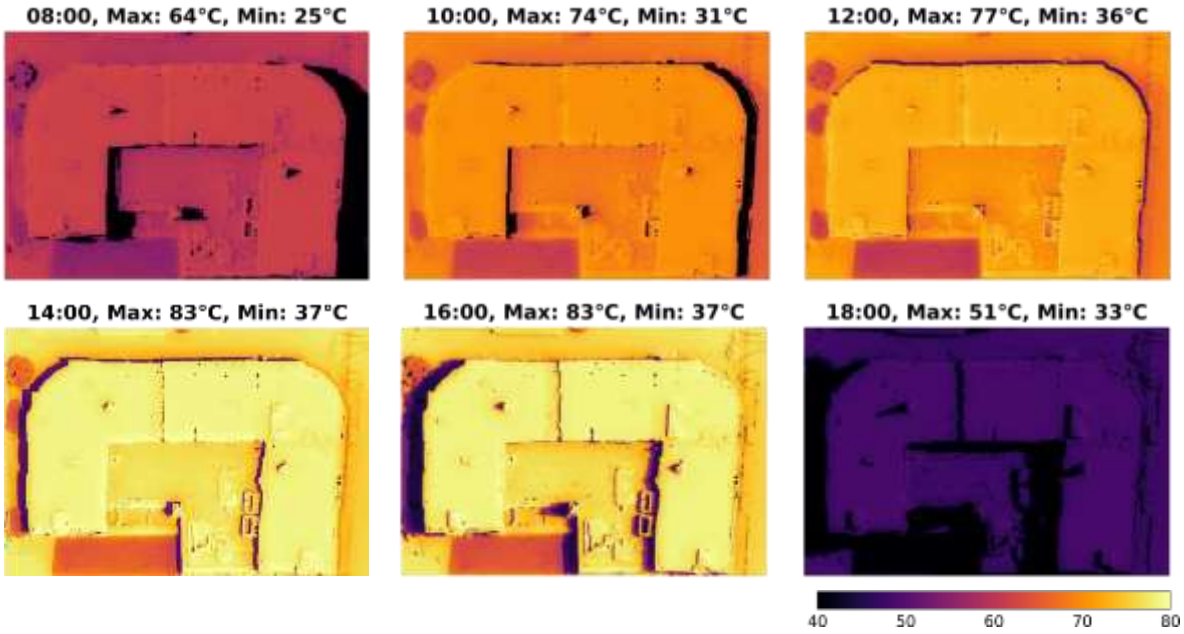

Figure 4. Spatial analysis of T_{mrt} on 7/17/2022 (8:00~20:00).

The results of the hourly site-scale heat stress assessment are depicted in Figure 5, including minimum WBGT, maximum WBGT, mean WBGT, and HI. According to NIOSH standards (Jacklitsch et al. 2016), WBGT values between 25.6-27.8°C are classified as 'Heat category 1', and WBGT values between 27.8-29.4°C are classified as 'Heat category 2'. The appropriate work/rest time and water intake strategies can be determined based on the heat category and type of work, as shown in Table 1. Based on the NWS standards, HI values between 26.7-32.2°C are categorized as 'Caution', and HI values between 32.2-39.4°C are classified as 'Extreme

Caution'. However, it is important to note that heat categories may vary depending on the location and thermal conditions. HI, while useful, has limitations as it cannot account for the spatial variations of heat radiation and only uses T_a and RH. The results demonstrate the existence of varying heat stress levels across the construction site, which is difficult to be captured by using the current on-site measurement methods alone. The proposed framework provides an effective solution to address this issue, enabling prioritization of high-risk areas and implementations of data-driven heat mitigation strategies such as hydration and optimized work and rest periods.

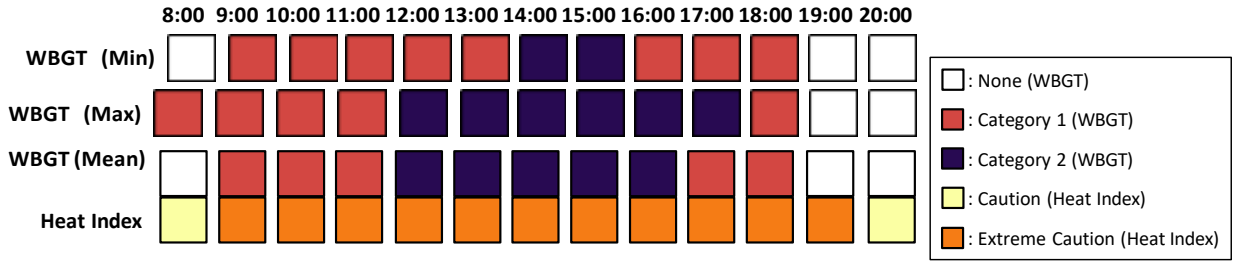

Figure 5. Hourly heat risk based on WBGT and Heat Index on 7/17/2022 (8:00~20:00).

Table 1. Recommendations based on the NIOSH standards in our study.

Heat Category	WBGT (°C)	Easy work (250 W)		Moderate work (425 W)		Hard work (600 W)	
		Work/Rest (min)	Water intake ($qt \cdot h^{-1}$)	Work/Rest (min)	Water intake ($qt \cdot h^{-1}$)	Work/Rest (min)	Water intake ($qt \cdot h^{-1}$)
1	25.6-27.8	Unlimited	0.5	Unlimited	0.75	40/20	0.75
2	27.8-29.4	Unlimited	0.5	50/10	0.75	30/30	1.0
3	29.4-31.1	Unlimited	0.75	40/20	0.75	30/30	1.0
4	31.1-32.2	Unlimited	0.75	30/30	0.75	20/40	1.0
5	32.2+	50/10	1.0	20/40	1.0	10/50	1.0

CONCLUSION

This study presents a novel method for evaluating heat risk in construction sites by combining UAV photogrammetry and microclimate simulation to identify previously overlooked radiant heat risks. The case study conducted in College Station, TX, demonstrates the effectiveness of the proposed framework. The proposed framework for assessing heat risk in construction sites combines meteorological, geometric, and thermophysical factors to produce more accurate and comprehensive heat radiation measurements, thereby reducing uncertainties and improving the reliability of heat risk assessments. The significance of monitoring heat radiation is emphasized in the study, as the lack of such monitoring can lead to erroneous assessments of occupational heat risks. This is due to the spatial variation of heat radiation, which poses a challenge to the current on-site measurement methods. The spatial variation of heat radiation can result in incorrect assessments of the occupational heat risks, making it crucial

to accurately monitor heat radiation to ensure the safety and health of construction workers. Future research will aim to implement the framework for heat risk management in construction and examine its benefits and limitations, with a focus on longer time frames, diverse site geometries, and varying meteorological conditions.

APPENDIX

Hourly results of case study on 7/17/2022 (8:00~20:00).

LST	T_a (°C)	RH (%)	V_a (m/s)	GHI (W/m^2)	Heat Index (°C)	T_{mrt} (°C)			WBGT (°C)		
						Mean	Min	Max	Mean	Min	Max
8:00	29.9	54.4	4.5	455.3	31.6	57.5	25.7	64.9	25.5	25.0	25.7
9:00	32.7	38.8	4.4	649.2	33.1	64.5	53.3	70.4	26.1	25.9	26.2
10:00	35.2	29.8	4.1	806.0	34.9	67.2	31.9	74.7	26.8	26.1	26.9
11:00	36.8	25.9	3.9	904.8	36.4	69.4	34.0	77.4	27.4	26.7	27.6
12:00	37.7	24.9	3.7	885.7	37.5	70.0	36.9	77.6	27.9	27.2	28.1
13:00	38.6	23.7	3.9	921.7	38.4	72.6	41.0	79.9	28.4	27.7	28.6
14:00	39.2	22.5	4.1	793.7	39.0	75.3	37.9	83.7	28.6	27.8	28.8
15:00	39.4	21.8	4.6	629.7	39.0	74.9	38.5	84.1	28.5	27.8	28.8
16:00	39.1	21.8	5.2	498.2	38.6	73.5	37.3	83.6	28.2	27.6	28.5
17:00	38.2	23.0	5.8	329.0	37.6	68.1	35.8	79.1	27.7	27.1	27.9
18:00	36.3	26.7	6.0	62.5	35.8	45.4	33.2	52.0	26.6	26.4	26.7
19:00	33.7	32.4	5.4	7.8	33.3	38.8	29.8	47.0	25.4	25.3	25.5
20:00	31.0	38.7	4.4	0.0	30.7	25.1	24.8	26.9	23.9	23.9	23.9

ACKNOWLEDGEMENT

This material is in part based upon work supported by the National Science Foundation (NSF) under Award #2126045. Any opinions, findings, and conclusions or recommendations expressed in this material are those of the authors and do not necessarily reflect the views of the NSF.

REFERENCES

Acharya, P., B. Boggess, and K. Zhang. (2018). "Assessing Heat Stress and Health among Construction Workers in a Changing Climate: A Review." *IJERPH*, 15 (2): 247.

Chan, A. P. C., M. C. H. Yam, J. W. Y. Chung, and W. Yi. (2012). "Developing a heat stress model for construction workers." *Journal of Facilities Management*, 10 (1): 59–74.

Chen, L., B. Yu, F. Yang, and H. Mayer. (2016). "Intra-urban differences of mean radiant temperature in different urban settings in Shanghai and implications for heat stress under heat waves: A GIS-based approach." *Energy and Buildings*, 130: 829–842.

Dong, X. S., G. H. West, A. Holloway-Beth, X. Wang, and R. K. Sokas. (2019). "Heat-related deaths among construction workers in the United States." *Am J Ind Med*, 62 (12): 1047–1057.

Fang, Z., T. Tang, Z. Zheng, X. Zhou, W. Liu, and Y. Zhang. (2021). "Thermal responses of workers during summer: An outdoor investigation of construction sites in South China." *Sustainable Cities and Society*, 66: 102705.

Huang, J., Y. Chen, P. Jones, and T. Hao. (2022). "Heat stress and outdoor activities in open spaces of public housing estates in Hong Kong: A perspective of the elderly community." *Indoor and Built Environment*, 31 (6): 1447–1463.

Jacklitsch, B., W. J. Williams, K. Musolin, A. Coca, J.-H. Kim, and N. Turner. (2016). *Occupational exposure to heat and hot environments*. Department of Health and Human Services, Centers for Disease Control and Prevention, Criteria for a Recommended Standard.

Kántor, N., and J. Unger. (2011). "The most problematic variable in the course of human-biometeorological comfort assessment — the mean radiant temperature." *Open Geosciences*, 3 (1): 90–100.

Lai, D., D. Guo, Y. Hou, C. Lin, and Q. Chen. (2014). "Studies of outdoor thermal comfort in northern China." *Building and Environment*, 77: 110–118.

Lau, K. K.-L., C. Ren, J. Ho, and E. Ng. (2016). "Numerical modelling of mean radiant temperature in high-density sub-tropical urban environment." *Energy and Buildings*, 114: 80–86.

Lindberg, F., and C. S. B. Grimmond. (2011). "The influence of vegetation and building morphology on shadow patterns and mean radiant temperatures in urban areas: model development and evaluation." *Theor Appl Climatol*, 105 (3–4): 311–323.

Lindberg, F., B. Holmer, and S. Thorsson. (2008). "SOLWEIG 1.0 – Modelling spatial variations of 3D radiant fluxes and mean radiant temperature in complex urban settings." *Int J Biometeorol*, 52 (7): 697–713.

Lindberg, F., S. Onomura, and C. S. B. Grimmond. (2016). "Influence of ground surface characteristics on the mean radiant temperature in urban areas." *Int J Biometeorol*, 60 (9): 1439–1452.

Stull, R. (2011). "Wet-Bulb Temperature from Relative Humidity and Air Temperature." *Journal of Applied Meteorology and Climatology*, 50 (11): 2267–2269.

Szer, I., T. Lipecki, J. Szer, and K. Czarnocki. (2022). "Using meteorological data to estimate heat stress of construction workers on scaffolds for improved safety standards." *Automation in Construction*, 134: 104079.

Wong, D. P., J. W. Chung, A. P. Chan, F. K. Wong, and W. Yi. (2014). "Comparing the physiological and perceptual responses of construction workers (bar benders and bar fixers) in a hot environment." *Applied Ergonomics*, 45 (6): 1705–1711.

Yi, W., A. P. C. Chan, X. Wang, and J. Wang. (2016). "Development of an early-warning system for site work in hot and humid environments: A case study." *Automation in Construction*, 62: 101–113.